Supplementary Information

Intelligent machines work in unstructured environments by differential neuromorphic computing

Authors

Shengbo Wang[†1], Shuo Gao[†*1], Chenyu Tang[2], Edoardo Occhipinti[3], Cong Li[1], Shurui Wang[1], Jiaqi Wang[1], Hubin Zhao[4], Guohua Hu[5], Arokia Nathan[6], Ravinder Dahiya[7], Luigi Occhipinti[*2]

Affiliations

[1]School of Instrumentation and Optoelectronic Engineering, Beihang University, Beijing, China

[2]Department of Engineering, University of Cambridge, Cambridge, UK

[3]Department of Computing, Imperial College London, UK

[4]HUB of Intelligent Neuro-engineering (HUBIN), CREATe, Division of Surgery and Interventional Science, UCL, HA7 4LP, Stanmore, UK

[5]Department of Electronic Engineering, The Chinese University of Hong Kong, Shatin, N. T., Hong Kong S. A. R., China

[6]Darwin College, University of Cambridge, Cambridge, UK

[7]Bendable Electronics and Sustainable Technologies (BEST) Group, Department of Electrical and Computer Engineering, Northeastern University, Boston, MA 02115, USA

[†]These authors contributed equally to this work

[*]Correspondence to: shuo_gao@buaa.edu.cn, lgo23@cam.ac.uk

Table of Contents

Discussion

1. Requirements for next-generation intelligent machines

In the working process of intelligent machines, there are three core parts: perception, processing, and execution. Among these, perception is particularly important because it provides basic raw data. However, as intelligent machines venture into unknown environments, building an effective perception system for these unfamiliar external environments has become an urgent problem to solve. This is particularly important for machines designed for extreme adventures, where the detection accuracy of external damage signals significantly impacts the quality of services rendered and their overall lifespan (*1–3*).

In unknown environments, intelligent machines often interact with the environment and objects that have unknown attributes and complex features. This necessitates the need for intelligent machines to possess comprehensive perception abilities, which refers to the ability to fully understand the main information in the environment, extract the key features, and preprocess it accordingly. The perception method should be scalable and generalizable, allowing intelligent machines to perceive and understand information in different modalities (including vision and touch) and adapt flexibly to unlearned or unexperienced scenarios or stimuli. When an intelligent machine lacks comprehensive perception ability, key features of the object can be lost during the perception process, resulting in poor interactions. For example, in robot grasping, if an unknown object has a smooth surface and is fragile, the lack of perception of the smooth surface characteristics may lead to an excessive force being applied during grasping, potentially damaging its structure. Therefore, it is crucial for intelligent machines to possess comprehensive perception abilities (*4–6*).

Biology possesses this comprehensive perception ability to perceive the external world. During the process of biological perception, various sensory receptors (such as nociceptors, fast-adapting receptors, and slow-adapting receptors) work in synergy with neurons to extract key features from external stimuli and carry out corresponding preprocessing. For example, in tactile information perception, nociceptors help organisms recognize harmful stimuli such as mechanical stress and extreme temperatures, enabling them to swiftly initiate motor reflexes. Meanwhile, adapting receptors can adapt to milder stimuli and reduce computational load. This structure of the perception method is scalable, not only for tactile information but also for visual and auditory stimuli. By extracting features from raw sensory information and differentiating processing through distinct neural pathways, this method allows us to adapt to the external environment in a highly generalized manner rather than being limited to specific scenes or objects.

In conclusion, this highly efficient perception mechanism serves as a valuable reference for the advancement of future intelligent machines. We aspire to equip these intelligent machines with a comprehensive perceptual capability akin to that of living organisms, enabling them to better comprehend environmental information.

2. The challenges of unstructured working environments and current research overview

Considering the requisites outlined for contemporary robots in the previous discussion section 1**,** it becomes evident that these requisites primarily arise from the development trend of intelligent machines. This trend extends from controlled laboratory and factory environments to include dynamic home and business environments, characterized by heightened unpredictability. These environments, often referred to as unstructured environments, present challenges to a robot's ability to perceive its surroundings. In this section, we start by exploring the definition of unstructured environments to gain a comprehensive overview of the attributes of working environments for future robotics. Subsequently, we will discuss the challenges posed by unstructured environments, focusing specifically on grasping and autonomous driving tasks. Furthermore, we review current research efforts aimed at addressing these challenges associated with unstructured environments.

2.1 The definition of unstructured working environments

Unstructured environments refer to environments that are not prearranged or modified to facilitate a robot's task execution. These environments consist of various objects and interaction scenarios where the robot lacks prior knowledge of object and environment properties. For instance, in robot grasping scenarios, traditional industrial robots operate in structured environments where they have prior knowledge of object properties (geometric shapes, masses, friction coefficients, etc.), whereas in unstructured environments, the contact properties of objects are completely unknown and highly variable, posing significant challenges for robots operating in such unpredictable surroundings (*7*, *8*).

2.2 Detailed challenges in grasping and autodriving

In this section, we will discuss the impact of unstructured environments on two specific tasks: grasping and autodriving.

2.2.1 Grasping

In a structured environment, the robot possesses precise information about the position and shape of the object to be grasped, which can be described using a straightforward mathematical model. Consequently, the entire grasping task benefits from well-defined modeling assumptions,

enabling the robot to establish its grasping plan with precision. Nonetheless, in unstructured environments, the variety of objects to be grasped is extensive, and their contact properties remain unknown. As a result, there is no explicit mathematical model available, rendering precise grasping planning unfeasible in such unstructured settings. To address the uncertainties posed by unstructured environments during the grasping process, it is crucial to enable the robot to acquire and comprehend object properties. This perception needs to be robust, generalizable, and capable of sensing multiple properties of the object. Furthermore, it should assist the robot in adjusting its grasping strategy, including the mode and force control, based on the learned sensory information. This adaptive approach is essential for enhancing the robot's performance in unstructured environments (*9–12*).

2.2.2 Autodriving

In structured environments, the driving process benefits from prior knowledge, such as the expected appearance of objects and their corresponding motion trajectories. Additionally, structured environments are more deterministic and often characterized by explicit map and road information. Conversely, there is a lack of a priori knowledge and high levels of uncertainty in unstructured environments, which encompasses variables such as unknown obstacle locations and the erratic movement of dynamic obstacles. This complex and uncertain nature of unstructured environments demands a strong visual perception capability for autonomous driving. One crucial requirement is the swift detection and screening of dynamic obstacles and environmental information, which facilitates the system's decision-making process, ensuring driving safety and enhancing environmental understanding (*13–15*).

2.3 The current research

When external environmental information is dynamic and unstructured, perceiving and comprehensively understanding this information requires a significant amount of storage and computation. Conventional intelligent machines operate within the von Neumann separated storage and computation architecture, leading to transmission bottlenecks and processing delays. However, memristors, devices with the ability to simultaneously store and process information, are well-suited for real-time sensing and processing of unstructured information in unknown environments. This similarity opens up the possibility of achieving comprehensive perception ability in intelligent machines (*16–18*). This section will review the work on memristor-based environment perception in intelligent machines.

The current memristor-based tactile perception method mainly focuses on imitating biological receptors, particularly nociceptors (*19–21*). Yoon et al. implemented a biological nociceptor with a thermoelectric module, a memristor, and a resistor in series with the memristor. The thermoelectric module acts as the external signal source, generating voltage pulses of different amplitudes

depending on external thermal stimuli (*22*). The conductance of the memristor changes with the voltage pulses, and the voltage characteristics observed from the resistor define key functions of the biological nociceptor, such as "threshold," "relaxation," "no adaptation," "sensitization," and "cure." Similarly, Kim et al. demonstrated a solid-state nociceptor based on a Pt/HfO_2/TiN memristor with the functions of threshold, relaxation, allodynia, and hyperalgesia. In their design, a p-FET was considered to be the spinal cord, which amplifies the output signal of the nociceptor (*23*). However, a major limitation of these efforts is that they primarily focus on emulating individual biological receptors using a single memristor, which may result in the loss of key environmental features and limit the ability to achieve a comprehensive understanding of environmental information.

In terms of visual perception systems, memristors can map external image information to its conductance. Similar to the tactile perception system, visual perception systems can be demonstrated by connecting light-sensitive devices to ordinary memristors. Light-sensitive devices convert optical signals to electrical signals, which can trigger the switching of memristors (*24*, *25*). However, these works primarily focus on converting visual information, and there is still a gap in regard to enabling intelligent machines to comprehend the environment. In the field of neuromorphic computing (where devices are not limited to memristors), inspired by biological rod cells, Zhang et al. designed a neuromorphic moving object detection system (*26*). The system operates by comparing two frames of visual information to identify disparities. However, it is not well suited for real-world autonomous driving scenarios. Slow background changes can introduce noise interference when swiftly detecting and screening dynamic obstacles and environmental information. Das et al. imitated the biological lobula giant movement detector (LGMD) neuron to detect driving collisions with a blue light-emitting diode (LED) as the optical source (*27*). Through designing the programming stimulation, they realize a photoreceptor that can generate a similar escape response in LGMD neurons used to detect collisions. However, in real-world scenarios, the lighting environment is intricate, and there is a disparity exists between the actual environment and the hypothetical environment used for collision detection.

In summary, intelligent machines still require a method that can equip them with comprehensive perception capabilities and enable them to exhibit high performance in real-world scenarios.

3. Differential sensory processing in biology and its advantages.

To address the current issues with memristor-based biological environmental information perception systems, we will first discuss the structural framework for processing unstructured environmental data in biological systems. Next, we will delve into the core perceptual mechanisms

involved and conduct a comparative analysis to elucidate the distinct advantages of the biological core perception mechanism (the sensory information differentiation and learning mechanism).

3.1 The structure of biological sensory systems

Biological sensory systems play a crucial role in gathering information from the surroundings and transmitting it to the central nervous system, enabling behavior and physiological responses (*28–30*). Commonly recognized systems include touch, vision, and hearing. These sensory systems consist of sensory neurons (sensory receptors), neural pathways, and parts of the brain involved in sensory perception. When exposed to external stimuli, receptors simultaneously encode and transform the stimuli into action potentials, which are then understood and processed differentially by the nervous system. After this conversion, the action potentials or signals are transmitted along dedicated neural pathways to the central nervous system. These pathways are composed of chains of neurons that relay information from one neuron to another, eventually reaching the appropriate regions of the brain for further processing. For example, visual information reaches the visual cortex, while auditory information targets the auditory cortex, and so on. Subsequently, the brain interprets and integrates the sensory input, allowing us to perceive and understand our environment. This interpretation of sensory information performed by the brain is defined as perception.

3.2 Differential sensory processing in the sensory system

The sensory information differentiation processing and learning mechanism is the most important processing mechanism for the biological perception of unstructured environmental information (*31–35*). This differentiation is reflected in two aspects, the encoding of external sensory stimuli by receptor neurons and the processing and learning of the encoded information by neural pathways. The encoding mainly refers to the specificity of the receptor neuron in response to the same stimulus; for example, the nociceptive receptor only responds to the dangerous stimulus specifically. This process of differential response is essentially the extraction of features from the current stimulus. During this perception process, organisms utilize the differentiation of sensory neural responses to encode different features and perceive the multidimensional features of the external stimulus. Subsequently, the encoded neural pulses are processed by different subsequent neural pathways, which typically have different structures and synaptic connection weights, representing subsequent differential processing and learning functions (*36–39*).

3.3 The differential sensory process model

From the onset of external stimulus action to encoding into neural impulses, the model can be classified into two stages. The first stage can be envisioned as a filter stage, where the sensory stimulus is filtered based on the feature selectivity of a given neuron. The second stage serves as an

input-output stage, transforming the filtered stimulus input into a firing rate output. Different receptor neurons initially exhibit variability in feature selection, manifested by their ability to extract various features from the same stimulus. Subsequently, they encode the input feature information into neural impulses based on these features. The encoding process also displays variability, primarily influenced by the properties of the receptor neurons themselves. Ultimately, the neural pathways will process these encoding stimuli differentially.

3.4 Advantages

This differential processing and learning mechanism enables organisms to perceive multiple features of external stimuli in unstructured environments and perform different processing functions accordingly, thus allowing them to clearly understand unknown environments. For example, in tactile perception, multiple afferents with different response characteristics are utilized to actively perceive environmental features, including the shape, the material and the roughness of contacting objects, providing information to support our subsequent decision-making. Similarly, in visual perception, our visual afferents exhibit frequency differentiation for processing visual information, aiding in the filtration of rapidly changing objects.

4. Mathematical proof of the advantages of differential neuromorphic computing

For the local system of a single memristor, it is assumed that the external input is s, the conductance of the memristor is G, and the output is y. The input and output relationship can be expressed as:

$$y = h(s,G) = L(s,G) + |E(s,G)|$$

where $L(s,G)$ is the linearization of the $h(s,G)$ function as $s = s_0$ and $G = G_0$, $|E(s,G)|$ the error after $h(s,G)$ is linearized.

Suppose that $h : D \subset R^2 \to R$, and the function y has a first-order differential and a second-order differential; we obtain

$$|E(s,G)| \le \frac{1}{2} M(|s - s_0| + |G - G_0|)^2$$

where $M = \max\{|f_{xx}|, |f_{GG}|, |f_{xG}|\}$. Generally, the $h(s,G)$ function is a linear operation or a multiplication and division operation; thus $M \le 0$ and $M \ge 0$. As a result, $M = 0$ and $|E(s,G)| = 0$.

Thus, we have

$$y = h(s,G) = L(s,G) = h_x(s_0,G_0)(s - s_0) + h_G(s_0,G_0)(G - G_0) + h(s_0,G_0)$$

Then, we take the derivative with respect to y:

$$dy = L(s,G) - h(s_0,G_0) = h_x(s_0,G_0)(s - s_0) + h_G(s_0,G_0)(G - G_0)$$

As $G = G_0 + Z(\int Idt)$ and $dG = Z(I) = m(s)$, we obtain

$$dy = h_x(s_0, G_0)ds + h_G(s_0, G_0)m(s)$$

where I is the current passing through the memristor and Z is the relationship between the memristor conductance change and current. Generally, the current is relevant to current stimuli, thus there is a functional relationship m between s and dG.

When s, G, ds and m are fixed, dy is also determined. When the system adopts differential encoding, the function m is not fixed but is related to the characteristics of the external input at this time to realize various differentiation functions.

5. Differential modulation schemes for memristors

The implementation of a differential process and learning model for living beings can be conceptually divided into two computational phases. The first phase involves feature extraction and the encoding of sensory information, while the second phase is the differential processing of the feature information based on the memristors.

In the initial phase, the output signal from the sensor may manifest as either analog or digital. For analog sensor signals, feature extraction can be executed with analog/digital circuits, including the utilization of an analog filter to isolate high-frequency information from the current sensor or first employing an analog-to-digital converter for quantizing sensory data and then performing certain feature extraction operations. It is important to note that the use of analog circuits for feature extraction ensures real-time processing but may introduce potential signal transmission disturbances. In contrast, digital circuits offer performance characteristics opposite to those mentioned above. Next, for processing the feature information extracted based on memristors, it becomes imperative to encode this information into analog signals. If the feature information is already analog, some preprocessing steps (such as amplification or limiting) can be performed to prepare the encoded signal for processing by memristors in the second stage. However, if the feature information is originally in digital format, it is essential to convert it into analog signals before subjecting it to the signal processing steps outlined earlier.

The second stage involves the differential processing of feature information using memristors. This stage resembles the attainment of computational functions through the memristor's intrinsic ability to alter its resistance value in response to differential stimulus encoding. The distinctiveness of this processing function becomes more pronounced when the nature of the stimulus varies according to feature encoding. For instance, in the context of processing tactile information, stimuli associated with dangerous features are encoded as positive voltage pulses, while those related to mild features are encoded as negative voltage pulses. In the case of stimuli corresponding to the dangerous features, the memristor's conductance increases, whereas it decreases for stimuli

associated with mild features. Furthermore, given the memristor's role as a synaptic weight in transmitting sensory information, it possesses the capability to amplify dangerous stimuli and adjust to mild ones. This capacity enables the differential processing of information.

The sensory information differentiation learning mechanism is the most important processing mechanism for the biological perception of unstructured environmental information, which can be reflected in two parts: the encoding of external sensory stimuli by receptor neurons and the processing and learning of the encoded information by neural pathways. First, diverse receptor neurons generate specialized encodings when perceiving the stimulus. For example, the nociceptive receptor encodes the injury stimulus specifically while the adaptive receptor encodes the mild stimuli. This process of differential encoding is essentially the extraction of different features from the current stimulus. During this perception process, organisms utilize the differentiation of sensory neurons' responses to encode the different features, perceiving the multidimensional features of the external stimulus. Second, the encoded neural impulses are processed by different subsequent neural pathways, which typically have different structures and synaptic connection weights, enabling differential processing and learning functions.

6. Learning of external sensory information

The synapse-like characteristics of memristors offer intriguing possibilities for learning from external sensory information. In this perceptual approach, we encode environmental feature information as voltage stimuli, leading to changes in memristor resistance. Each specific state of the memristor represents the acquisition of distinct feature information. In our demonstration of tactile information perception, the memristor resistance adjusts according to the real-time attributes of the current external tactile stimulus. The memristor's state information at each moment reflects the cumulative effect of past stimulus history. For instance, a low memristor resistance value indicates that the robot has encountered potentially dangerous stimuli for an extended period, serving as a basis for the robot to trigger a pain reflex. This continuous learning capability enhances the robot's autonomy, particularly in unfamiliar environments (*43*).

Similarly, in the realm of visual information processing, high-frequency visual data are encoded as positive voltage pulse stimuli, with pulse amplitude escalating in proportion to the degree of variation. Consequently, memristors with lower resistance values exhibit heightened sensitivity to high-frequency changes in light intensity within a given region. This heightened responsiveness is of paramount significance for real-time decision-making, particularly in autonomous driving scenarios. In conjunction with the extraction of environmental feature information, memristors can proficiently acquire a multifaceted understanding of the surroundings,

making them exceptionally well suited for intelligent machines functioning in unstructured environments.

7. Biological tactile sensory system implementation based on memristors

Within living organisms, multiple receptors play a pivotal role in detecting external tactile stimuli, resulting in intricate and nuanced tactile perception. In this section, we elucidate how organisms differentially process and acquire tactile information and demonstrate how our methodology can be applied to attain biomimetic perception.

7.1 Biological differential processing and learning

Differential processing of tactile stimuli in organisms primarily encompasses two crucial functions: amplification of dangerous stimuli and adaptation to mild stimuli. The former is achieved through the engagement of nociceptors and their corresponding neural pathways, while the latter is orchestrated by fast-adapting and slow-adapting receptors, along with their respective neural pathways.

Nociceptors are the receptors responsible for sensing potentially dangerous sensory stimuli in living organisms (*44–47*). Through the subsequent neural pathways, they perform crucial functions, including 'threshold', 'no adaptation', 'sensitization' and 'relaxation'. The "threshold" refers to the condition where the nociceptor responds only when external tactile stimuli reach a certain threshold, typically possessing dangerous characteristics. 'No adaptation' means that the nociceptor consistently increases its response intensity to strong stimuli as it learns and assimilates the environmental danger information. 'Sensitization' signifies that after perceiving certain dangerous stimuli, the nociceptor enters a sensitized state, further intensifying its response to dangerous stimuli. The 'relaxation' indicates that when external dangerous stimuli are removed, the nociceptor returns to its normal state, reducing the level of sensitivity amplification to external stimuli back to its initial value. Based on these nociceptor functions, organisms can swiftly detect dangerous stimuli, ensuring their safety. These functions are necessary for intelligent machines operating in unknown environments.

In contrast, rapidly adapting receptors and slowly adapting receptors, along with their subsequent neural pathways, adapt to external stimuli by gradually reducing their response levels (*48–50*). These receptors are the key components in achieving sensory adaptation, a function primarily referring to the adaptation to mild external stimuli, which involves learning environmental information related to mild stimuli and continuously reducing their response intensity to such stimuli. Rapidly adapting receptors adapt to stimuli swiftly, whereas slowly adapting receptors do so at a more gradual pace. This perceptual mechanism aids in lightening the processing burden on the

central nervous system and enables the prompt detection of changes in stimuli. For instance, when the intensity of a mild stimulus undergoes a sudden alteration, it becomes more noticeable due to prior adaptation processing. Therefore, sensory adaptation also holds significant relevance in scenarios such as stable grasping in robotics.

7.2 Implementation based on memristors

In the perception of external tactile information, we utilize the current pressure magnitude as the stimulus input, considering the memristor as a synapse. The tactile response strength is determined by multiplying the stimulus input by the current relative conductance value of the memristor. The implementation of nociception and sensory adaptation is as follows:

For the processing of hazardous stimuli, we first evaluate whether the magnitude of the current pressure matches the criteria for dangerous features. Only when the current pressure surpasses a predefined threshold does the encoding unit generate positive voltage pulses, increasing the memristor's conductance. This corresponds to the ‘threshold’ function of biological nociceptors, as demonstrated in the following formula:

$$for \quad r(t) \subset r_d, \quad t_{sta} < t < t_{end}$$
$$v(t) = 0 \quad otherwise$$

where $v(t)$ represents the voltage stimuli applied to the memristor, and only if the pressure stimulus meets the hazard characteristics r_d is a voltage pulse with amplitude v_{noc} and duration from t_{sta} to t_{end} is generated. For continuous hazardous stimuli, the memristor's conductance gradually increases under sustained positive voltage stimuli, achieving ‘no adaptation’ to dangerous stimuli. The process can be represented as follows:

$$\frac{dx}{t} = f(x, v(t)) < 0$$

where x represents the memristor state. Under voltage pulses, the increase in the conductance of the memristor realizes the ‘no adaptation’ processing of the stimulus. Furthermore, to realize the ‘sensitization’ function, we draw inspiration from biology, where information from different time scales is simultaneously considered during processing. When the stimulus matches hazardous features and the memristor's conductance has already exceeded a certain threshold, it can be inferred that the robot has received hazardous stimulus information for a certain duration. At this point, we increase the amplitude of the positive voltage stimuli to further amplify the response to hazardous stimuli. When external stimuli are removed or no longer meet the hazardous criteria, the encoding unit re-encodes. Upon stimulus removal, the encoding unit generates recovery pulses, restoring the memristor to its initial resistance, achieving the ‘recovery’ function.

The processing of mild stimuli follows a similar procedure to that of hazardous stimuli. First, we extract and analyze the characteristics of external stimuli. When the tactile stimulus meets the

mild criteria (the force magnitude falls within a certain range), the encoding unit generates negative voltage pulses, reducing the memristor's conductance. When a mild stimulus remains stable within a range, the memristor's conductance continuously decreases, achieving adaptation to mild stimuli. This differentiation processing method allows us to adjust the adaptation speed by modifying the features of the encoding pulses based on mild characteristics, thereby emulating both rapidly adapting and slowly adapting receptors. When the force is removed or no longer meets the criteria for a mild stimulus, the encoding unit re-encodes. Upon stimulus removal, the memristor is reset to its initial setpoint resistance.

This differentiation processing method showcases multifunctional processing potential. In addition to the aforementioned biomimetic functions, we have also implemented normal perception functionality, which maintains the memristor resistance at a stable level i.e., it neither amplifies nor adapts to external stimuli. It is evident that this method holds great potential in processing unstructured tactile information. By further designing feature extraction logic and corresponding pulse encoding, robots can acquire multidimensional tactile sensing capabilities and improve their understanding of environmental information.

8. Biological visual sensory system and implementation based on memristors

The biological visual system consists of sensory organs (eyes) and parts of the central nervous system (sensory cells, optic nerves, optic tracts, and visual cortex). Through their coordinated efforts, living organisms are able to detect and interpret visual information. In this section, we will provide a detailed description of how biology processes and learns visual information, as well as the implementation of it on memristors we have achieved.

8.1 Biological differential processing and learning

In the process of human visual information perception, incoming light enters the eye and passes through a compound lens composed of the cornea and crystalline lens before being projected onto the retina. In the retina, two types of photoreceptor cells are involved in vision: rod cells and cone cells (*51–53*). These two classes of cells further transmit information to bipolar cells and ganglion cells, ultimately relaying it to the visual cortex, where visual perception occurs. Rod cells and cone cells exhibit distinct differentiation in their processing of light information. They differ in their sensitivity to light, with rod cells being highly sensitive to light and capable of functioning in dim lighting conditions, while cone cells are less light-sensitive and work in bright lighting conditions. Additionally, the time course of a light response is different between rods and cones: rods exhibit a sustained response to a flash of light, while cones show a brief response. This difference in response time affects the temporal resolution of rods and cones: cones are more effective than rods at

detecting high-frequency light flickering and are likely better suited for perceiving quickly moving objects. This differential processing and learning of light frequency information is crucial for detecting rapid changes in light intensity and distinguishing them from slower changes. In autonomous driving scenarios, the differential processing of light frequency information is also crucial for making timely driving decisions, leading the driver to respond appropriately.

8.2 Implementation based on memristors

In the proposed method, we initially use analog filters to extract changes in light intensity and generate corresponding encoding stimuli based on high-frequency and low-frequency characteristics. High-frequency light intensity information is crucial for real-time decision-making, whereas low-frequency information typically corresponds to slowly moving or stationary objects. To differentiate and learn the frequency features of visual information, we encode high-frequency information as positive voltage pulses and low-frequency information as negative pulses, causing corresponding changes in the memristor's resistance value. The stimuli encoded based on frequency can be represented by the following formula:

$$v(t) = m \times f_{light} + b > 0 \quad f_{light} \subset f_{high}$$
$$v(t) = n \times f_{light} + c < 0 \quad f_{light} \subset f_{low}$$

where f_{light} is the frequency information of the light intensity, f_{high} and f_{low} represent high-frequency and low-frequency change features, respectively, and the remaining parameters are constant coefficients. When the memristor exhibits a low-resistance state, it has effectively learned to detect high-frequency stimuli from the external environment. Consequently, executing emergency obstacle avoidance control in such circumstances is a reasonable course of action. Conversely, when the memristor is in a high-resistance state, it suggests that the changes in light intensity within that area have been gradual or slow.

9. The multisensory scalability of this differential perception method

By mimicking the intrinsic nature of human low-level perception mechanisms in electronic memristive neural circuits, the proposed differential perception method has the potential to process multimodal sensory information. In this discussion, we will discuss the principles of this method for processing multisensory information and its potential applications.

9.1 The principles of processing multisensory information

Expanding the perception method from single-sensory to multisensory information involves adjusting the front-end sensors to accommodate different types of physical stimuli. After obtaining the raw perceptual information through sensors, feature extraction and differentiation processing can still be applied to this sensory information, regardless of the original nature of the physical

stimuli. This scalability in perception is rooted in the fact that differentiation processing is a fundamental sensory mechanism in biology, existing across multiple senses and capable of handling stimuli with varying properties and quantities. In our proposed method, when the nature of external stimuli changes and the corresponding sensors are replaced, some modules can be fine-tuned, such as adjusting the voltage pulse amplitude generated by the encoding module, but the overall perceptual structure remains unchanged.

9.2 Outlook

Leveraging the scalability of our proposed perception method, intelligent machines can attain comprehensive perception abilities across diverse sensory inputs. When combined with various sensors, these intelligent machines can better comprehend environmental information through senses including touch, vision, and hearing, among others. Such perceptual and learning capabilities empower intelligent machines to excel in unknown environments by learning various environmental object features, addressing critical issues such as path planning, object recognition and grasping. Moreover, with the power of differential neuromorphic computing, intelligent machines can acquire human-like sensory abilities, allowing them to interact more naturally with humans. This includes perceiving and conveying information through speech, gestures, facial expressions, and sound, resulting in a better understanding and responsiveness to human needs. Furthermore, as intelligent machines continue to evolve, they will exhibit creative capabilities. Art and creativity frequently hinge on the ability to perceive the world and grasp its intricacies. When robots possess comprehensive perception abilities across multiple senses, including visual, auditory, tactile, olfactory, and gustatory information, they gain access to a wealth of input data, which becomes instrumental in observing and understanding the surrounding environment, human behaviors, and emotions. As a result, robots have access to a wider range of materials and background information to fuel their artistic and creative endeavors. Finally, intelligent machines hold the potential to surpass human capabilities. Combined with the Turing machine, intelligent machines not only possess efficient and sophisticated sensory capabilities akin to humans but can also quantitatively process sensory information to achieve virtually any computational functions, thereby surpassing the limitations of human abilities.

Supplementary Figures

Fig S1. The structure and properties of the piezoresistive film.

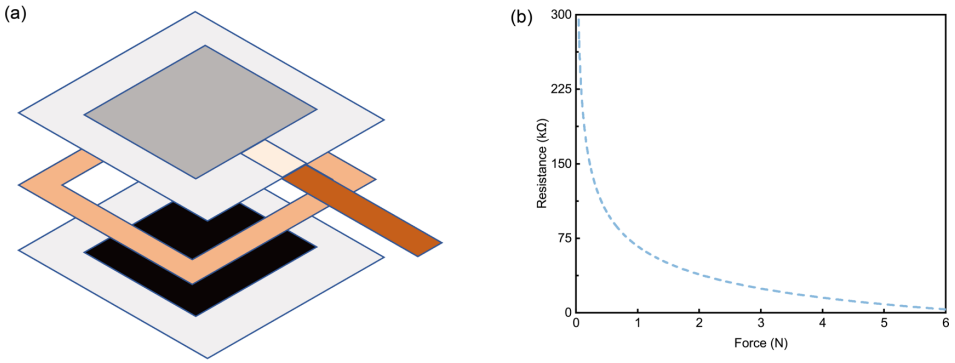

Fig S1. The structure and properties of the piezoresistive film. The specific structure of the device consists of the following layers: a protective layer of thermoplastic polyurethane elastomer rubber (TPU), a layer of conductive silver paste, a layer of pressure-sensitive material, and another layer of conductive silver paste, all enclosed between TPU protective layers. When external pressure is applied, the conductive silver paste makes contact with the pressure-sensitive material, enhancing conductivity and reducing the resistance of the device. Each point within the device can achieve a minimum resistance value of 10 kΩ, which increases to over 300 kΩ when no force is applied. In terms of performance, the piezoresistive film offers a wide range of force measurement capabilities, spanning from 0 to 6 N. The pressure characteristic curve exhibits a high degree of fitting. Specific fitting results can be observed in the figure.

Fig S2. The switching mechanisms of the self-directed channel (SDC) memristor.

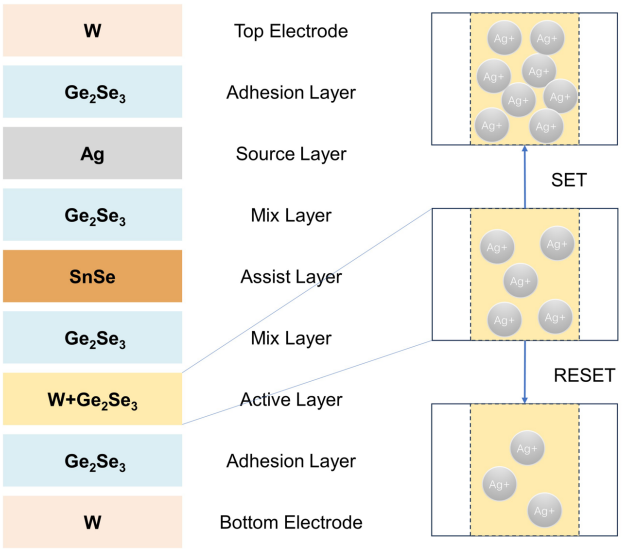

Fig S2. The switching mechanisms of the self-directed channel (SDC) memristor. Following fabrication, SDC devices start in a high-resistance state ranging from MΩ–GΩ. Upon first use of the device, the positive voltage applied to the top electrode can trigger the creation of the self-directed conductive channel in the SDC device. During this initial operation, Sn ions are generated from the SnSe layer and incorporated into the active Ge_2Se_3 layer. Theory suggests that these Sn ions promote the replacement of Ge by Ag at Ge-Ge bond sites in the active layer.

After Sn ions from the SnSe layer are incorporated into the Ge_2Se_3 layer, pairs of self-trapped electrons are produced within the Ge_2Se_3 layer. This process facilitates the replacement of Ge by Ag at the Ge-Ge bonds, creating "openings" near these bonds. These open regions serve as conduits for Ag^+ ions, allowing them to access the Ag-Ge sites and become natural "conductive channels" within the active layer during device operation.

The self-directed channel follows with the position of the initial Ge-Ge dimers in the glass, influenced by its inherent structure. Due to the tendency of Ag atoms to agglomerate, these specific sites can foster Ag accumulation within the glass. This accumulation results in varied Ag concentrations at these clustering points. Consequently, the device's resistance is primarily decided by the Ag concentration at a given site and the distance between agglomeration sites. By applying positive or negative potentials across the device, Ag can be moved onto or away from these agglomeration sites, allowing the resistance to be tuned in both lower and higher directions.

Fig S3. The control circuit for the memristor.

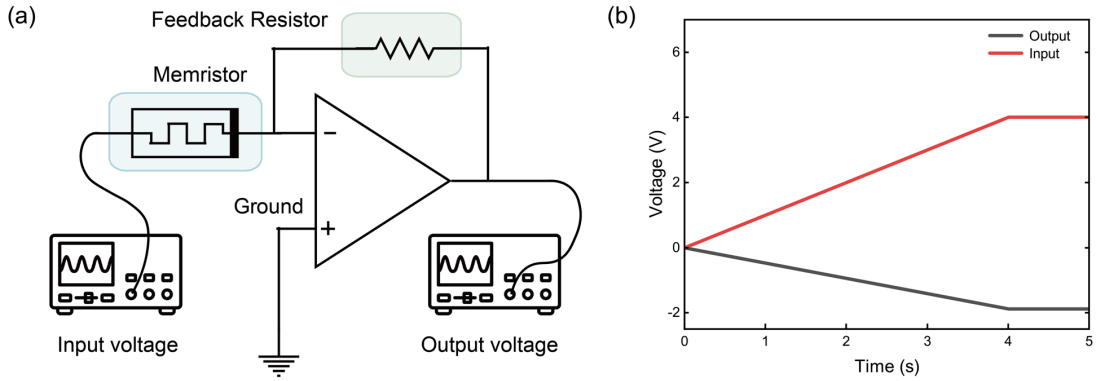

Fig S3. The control circuit for the memristor, based on the operational amplifier, is responsible for regulating the memristor state and providing feedback on its current state. The input terminal receives the encoded voltage from the signal generation module. By utilizing the negative feedback connection of the backend operational amplifier, the potential of the memristor bottom electrode is maintained at approximately 0 volts (virtual ground). This ensures that the voltage stimulus generated by the signal encoding remains undistorted and fully applies to both ends of the memristor, resulting in the modulation of the memristor. Moreover, the output voltage of the circuit allows for the feedback of the memristor state representing the long-term characteristics of the sensory stimuli.

Fig S4. The main system structure.

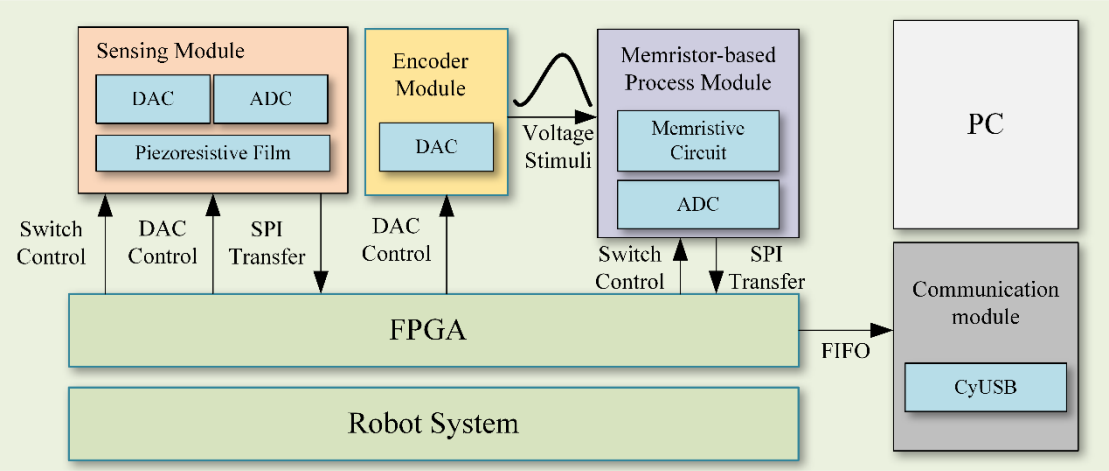

Fig S4. The main structure in tactile differentiation processing. The system is composed of several main components. The FPGA serves as the primary controller, with Intel's E4CE10F17C8 chosen as the FPGA main control chip. The external crystal oscillator operates at a frequency of 50 MHz. The front-end sensing module consists of a DAC, ADC, and piezoresistive film. The DAC is responsible for implementing neural coding to achieve differentiation encoding. The ADC, along with the memristor process circuit, forms the memristor neuromorphic processing module. To facilitate communication, the CY7C68013A chip works in conjunction with the PC host computer, enabling USB communication within the system. This setup enables the transmission of current perception information and the state information of the memristor's resistance value.

Fig S5. The system control schemes.

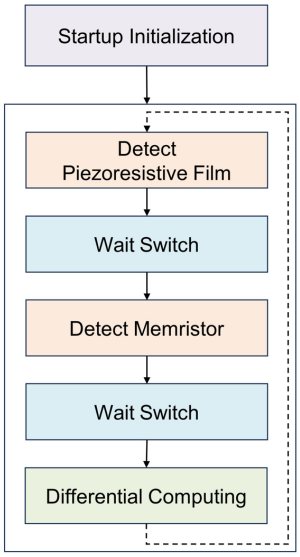

Fig S5. The control schemes in tactile differentiation processing. The system initiates by entering the initialization phase, where it performs an initial power-on reset on the device. Afterward, the system proceeds to the normal working cycle. Within each working cycle, the system first employs a digital-to-analog converter (DA) and an analog-to-digital converter (AD) to detect the resistance value of the piezoresistive film. It then waits for the system analog switch to activate after detection. Subsequently, it detects the resistance value of the memristor through the memristor read and write control circuit. Once both detections are completed, according to the differentiation logic, the DA circuits generate the corresponding differentiation voltage. This voltage is then used to modulate the resistance value of the memristor, achieving the differentiation calculation of pressure information.

Fig S6. The system background noise test.

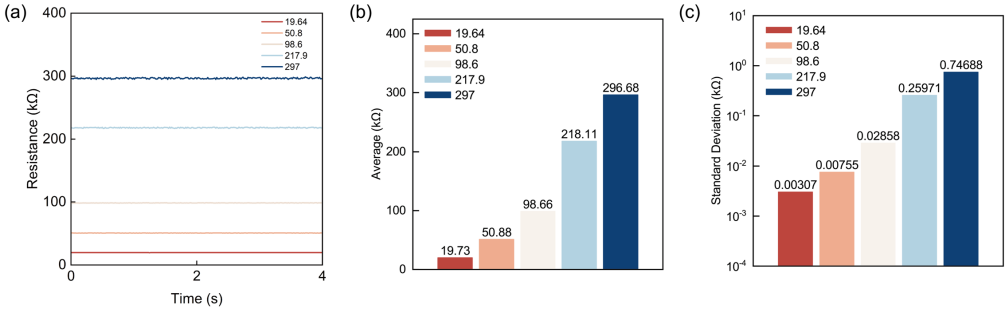

Fig S6. The system background noise test. (a) Measurement results of the fixed-value resistor. The memristor resistance device was substituted with a fixed-value resistor of varying values for testing purposes. By comparing the measured values with the actual values, it was observed that the overall system noise is relatively low. However, when testing a resistor with a high resistance value, it was found that the signal can be subject to fluctuations when exposed to noise. (b) The average value of the measured resistor. (c) The standard deviation of the measured resistor.

Fig S7. The different modulation types.

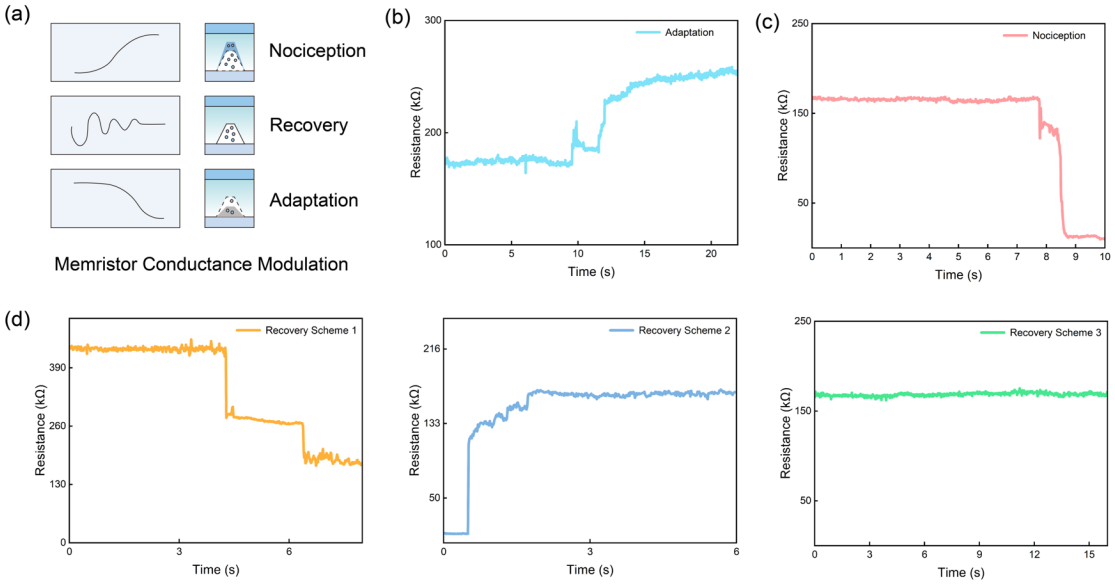

Fig S7. The memristor different modulation types. (a) In tactile information differential processing, there are three modulation modes: adaptation, nociception, and recovery. The amplitude of the modulation pulse of the adaptation type is negative, increasing the memristor resistance. In contrast, the amplitude of the nociception type is positive, decreasing the memristor resistance. The recovery pulse is responsible for resetting the memristor to the initial resistance interval; it is a negative pulse if the current state is low-resistance, a positive pulse if the current state is high-resistance, or no pulse is applied if it is already in the set interval. (b) The adaptation modulation pulse. (c) The nociception modulation pulse. (d) The recovery modulation pulse.

Fig S8. Tactile stimuli differential processing by biological receptors.

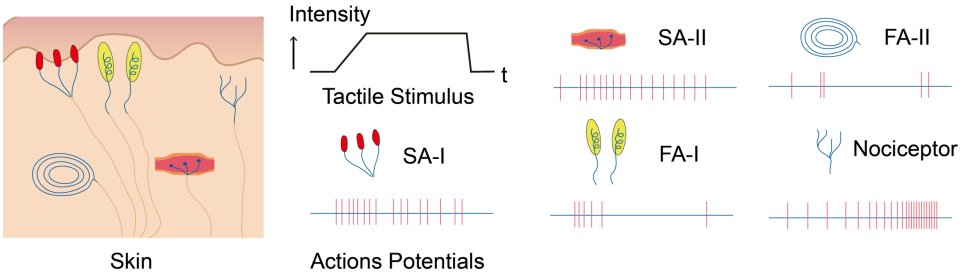

Fig S8. Differential processing of tactile stimuli by biological afferents. Two types, termed fast-adapting type I (FA-I) and fast-adapting type II (FA-II) afferents, respond only during dynamic phases of tissue deformation caused by tactile stimuli. Another two types, termed slowly adapting type I (SA-I) and slowly adapting type II (SA-II) afferents, respond to sustained skin deformation with graded sustained discharge. In addition, the nociceptor produces a sustained response to dangerous stimuli with increased intensity.

Fig S9. Other differential process functions.

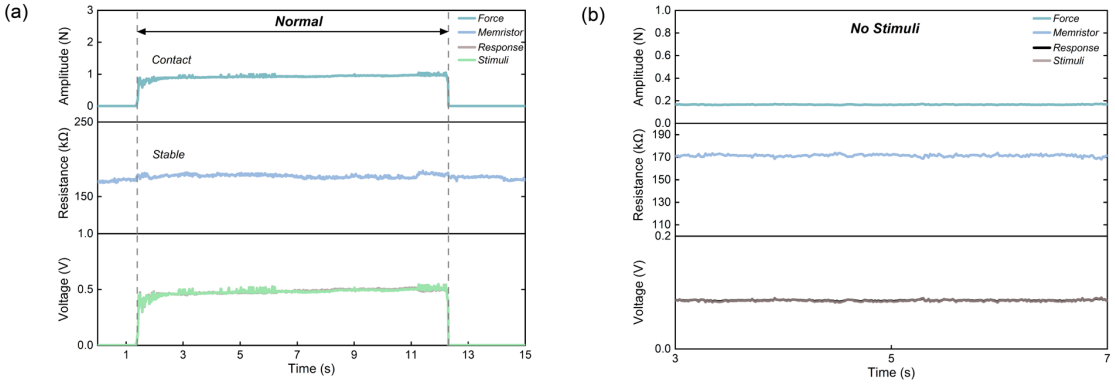

Fig S9. Other differential process functions. During actual tactile perception, there are scenarios where there is no need to amplify or adapt to external tactile stimuli. For instance, when there is no external tactile stimulus present (as depicted in Figure S9 b), modulating the memristor would result in unnecessary energy consumption. Similarly, in another case, when the external pressure has a specific intensity but does not require amplification and the system is desired to accurately perceive its real intensity, there is no need to modulate the resistance value of the memristor. This corresponds to the normal process function depicted in Figure S9 a.

Fig S10. Processing functions in dynamic scenarios.

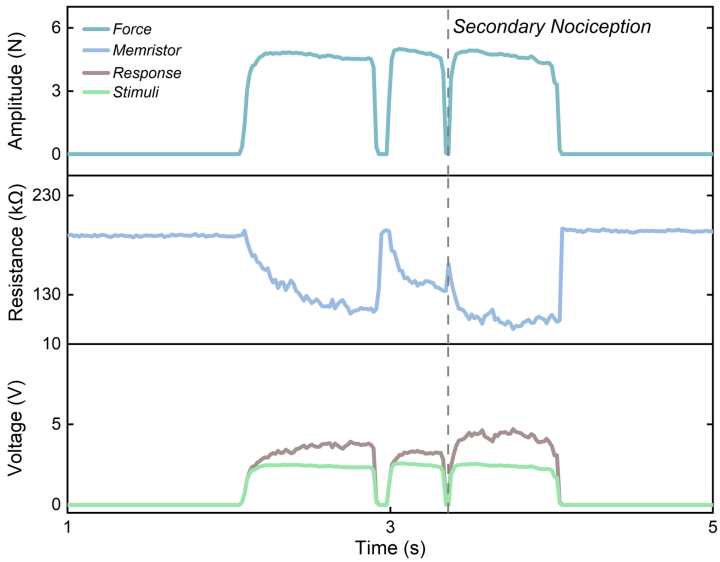

Fig S10. Processing functions in dynamic scenarios. In some dynamic scenarios, the features of the environmental information may change, and our proposed method is also capable of handling such dynamic information. As shown in Figure S10, when a dangerous stimulus is quickly withdrawn and then quickly applied again, the memristor resistance value has not yet reset completely. Thus, the memristor can achieve faster amplification of the external stimulus than that of the first stimulus, which demonstrates the function of 'secondary nociception'.

Fig S11. Control logic for pain reflex and slip detection.

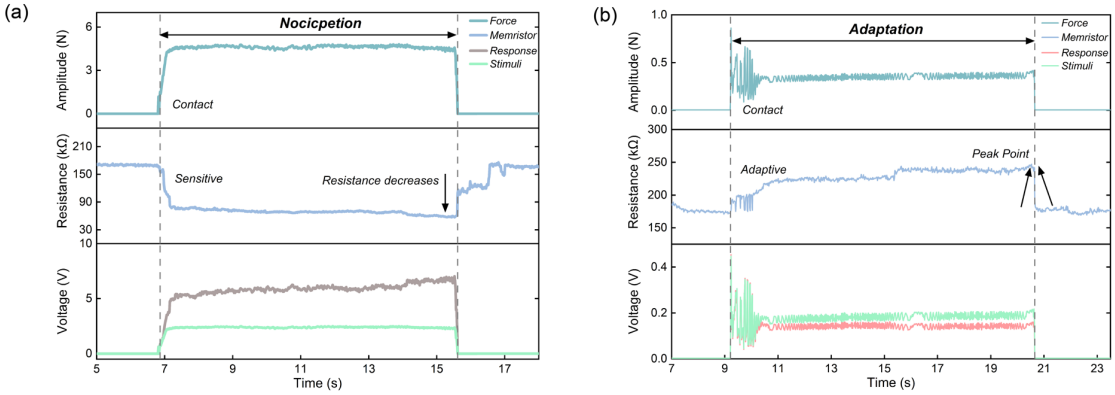

Fig S11. Control logic for pain reflex and slip detection. (a) The control logic for pain reflex. When working in unknown environments, robots need to have the ability to detect dangerous stimuli and provide a timely response. In such situations, the memristor is modulated to the low-resistance state under the positive pulses generated by the encoding module. When the memristor is less than a set threshold, it can be assumed that the robot has been subjected to dangerous stimuli for a period of time, and the pain reflex can be executed to protect the robot itself. (b) The control logic for slip detection. Once the robot has grasped the object to achieve stabilization, the slipping of the object primarily results from external interference. Thus, the memristor resistance will increase at first and decrease at the moment the object falls. The peak point of the memristor resistance will indicate the slipping of the object.

Fig S12. A memristor model used in visual information processing.

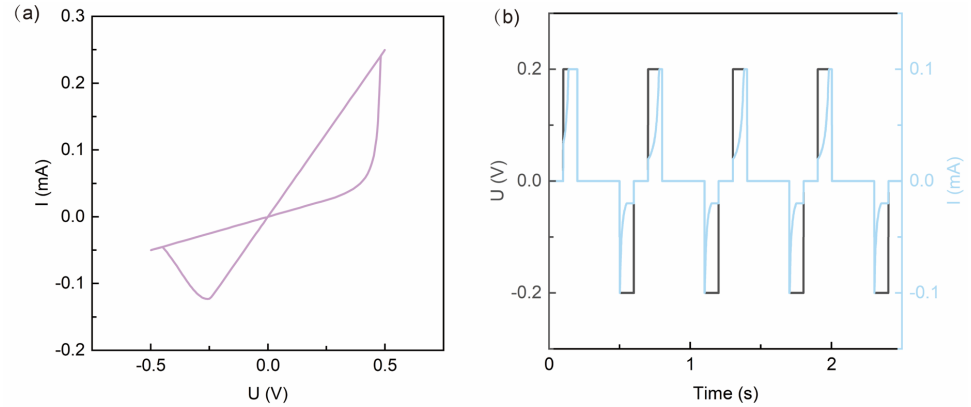

Fig S12. The voltage threshold adaptive memristor (VTEAM) model used in visual information processing. (a) The hysteresis curve of the memristor model. In this simulation, the tested sine wave has a peak-to-peak value of 1 V, and its frequency is 20 Hz. (b) The pulse test result of the memristor model. In this simulation, the amplitude of the pulse is 0.2 V, with a 0.1 s duration.

Fig S13. The circuit design of visual differential process system.

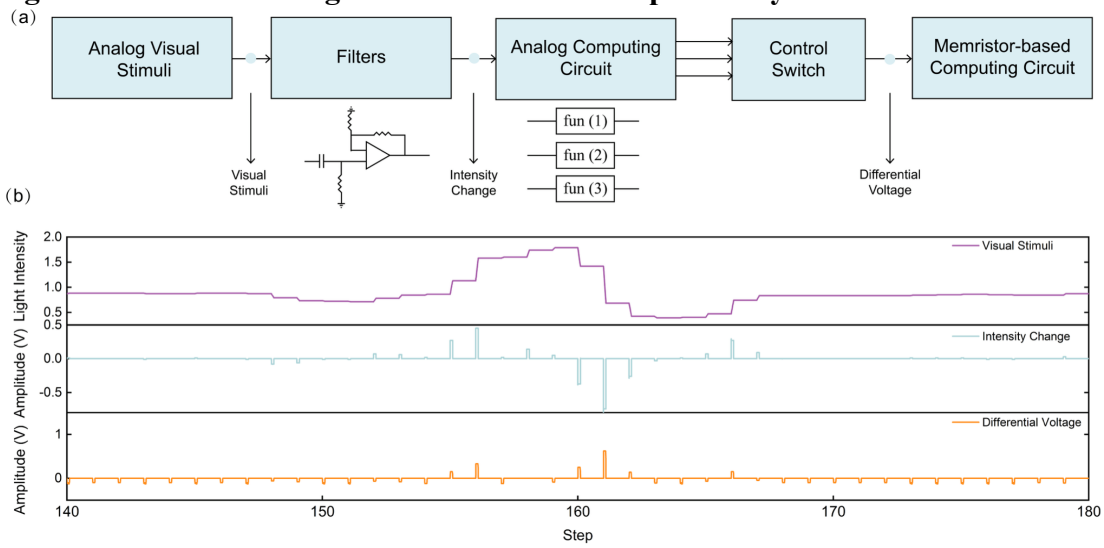

Fig S13. Circuit Design of the Visual Differential Process System. In this simulation, the external visual stimuli captured by the CMOS in-vehicle camera are utilized as the input signal for the system in the form of analog voltage signals. The visual information between two frames undergoes linear changes at a fixed time interval. Subsequently, the changes in visual information are extracted using filters. The extracted information is then differential into various voltage stimuli through the analog operation circuit. Finally, the differential voltage is applied to the memristor using the read and write control circuit.

Fig S14. Noise Testing of Vision Circuits.

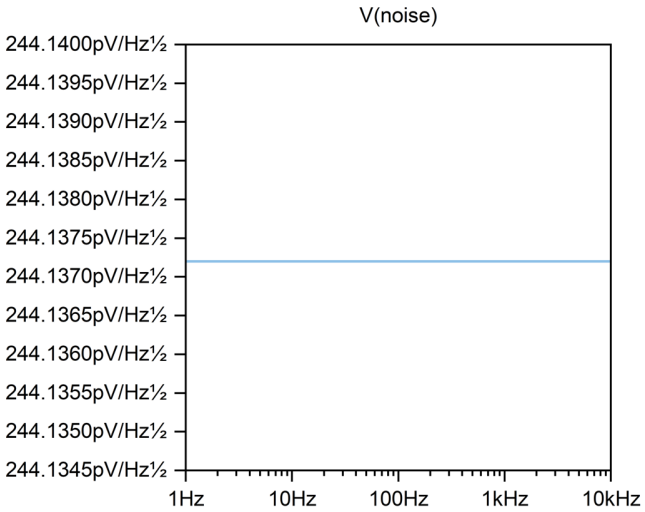

Fig S14. Noise Testing of Vision Circuits. To assess the noise levels in the vision circuits, we conducted a noise test. Assuming the external analog visual signal input is noise-free, we calculated the total noise that accumulates in the input voltage applied to the memristor read-write circuit. Through our calculations, we determined that the circuit noise level is approximately 200 pV.

Fig S15. The Influence of threshold selection on differentiation processing.

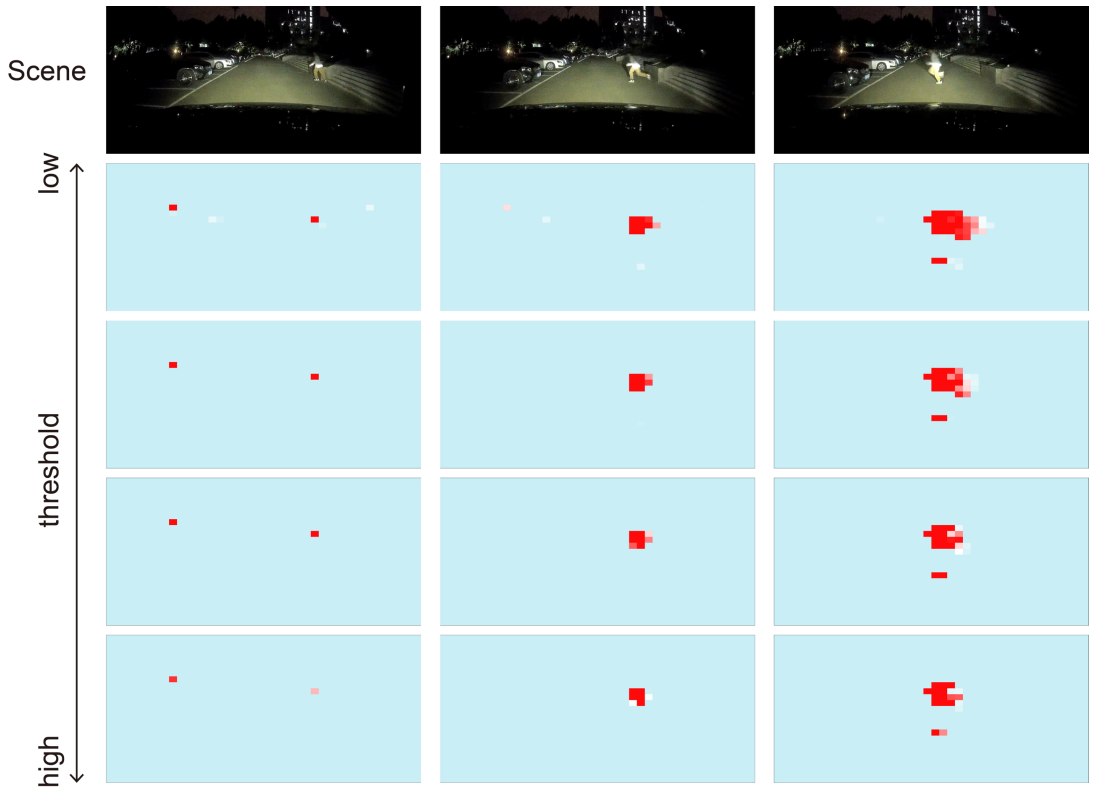

Fig S15. The influence of threshold selection in differentiation processing. In visual differentiation processing, the choice of threshold is pivotal in defining the properties of visual information. A positive voltage modulation scheme is generated only when the change frequency surpasses the threshold, leading the memristor into a low-resistance state. This signifies the presence of crucial object information during driving scenarios. As depicted in the accompanying figure, a higher selected threshold results in a smaller extracted area. However, the extracted information becomes more critical and pertinent. Concurrently, the duration of neural excitation is reduced with a high selected threshold. This is because a larger recovery negative voltage is more readily generated in this context.

Fig S16. The Impact of object distance on system detection performance.

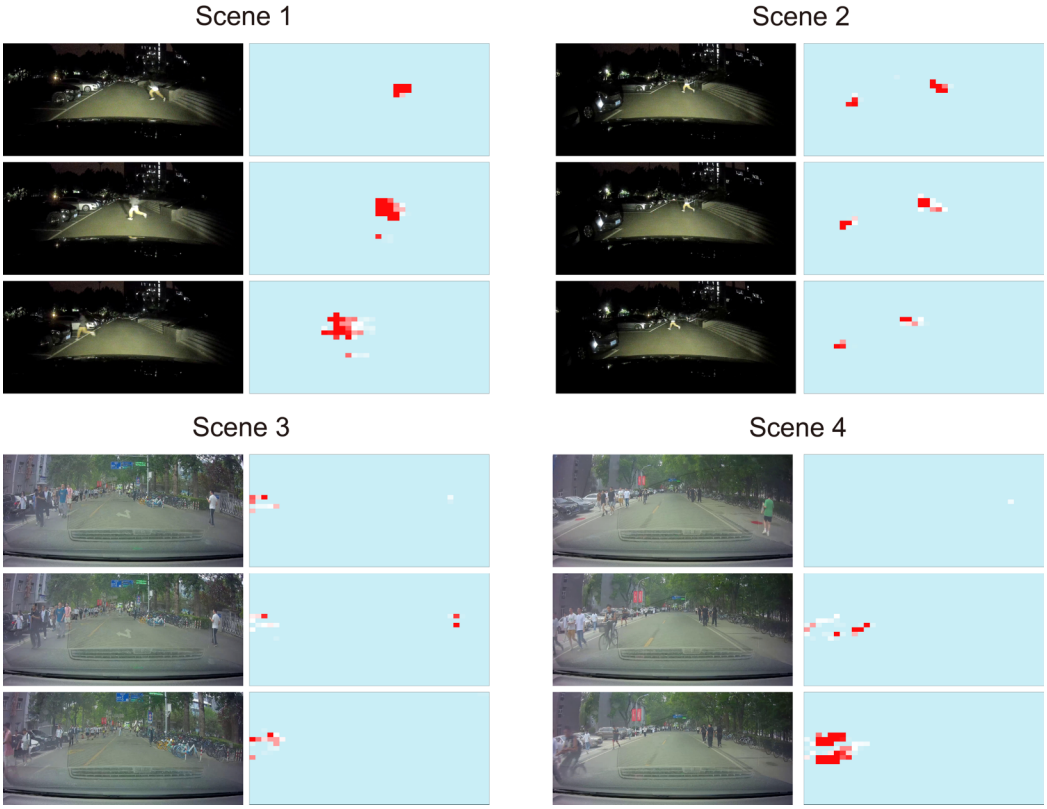

Fig S16. The impact of object distance on detection performance. The distance of objects within a compressed image influences their apparent size. Specifically, objects that are closer to the driver occupy a larger area in the image. As a result, nearby objects yield a larger extracted area than those that are distant, as demonstrated in Scene 1 and Scene 2. Moreover, an object moving at a constant speed becomes more detectable when it is closer, as illustrated by the comparison between Scene 3 and Scene 4.

Fig S17. Detection of road markings.

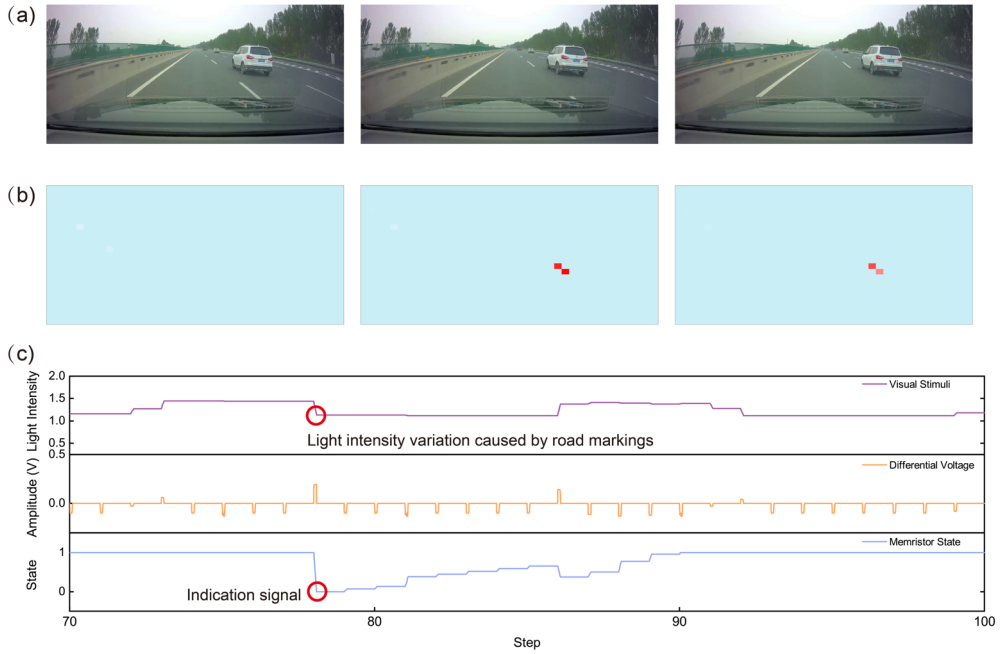

Fig S17. Detection of road markings. (a) Actual driving scenarios in the detection of road markings. While the road marking line itself remains stationary, the motion of a car induces relative movement, leading to variations in light intensity. This phenomenon enables the detection of the road marking line. (b) The detection results. (c) The light intensity change and its corresponding differential voltage and memristor state.

Fig S18. Detection of light sources.

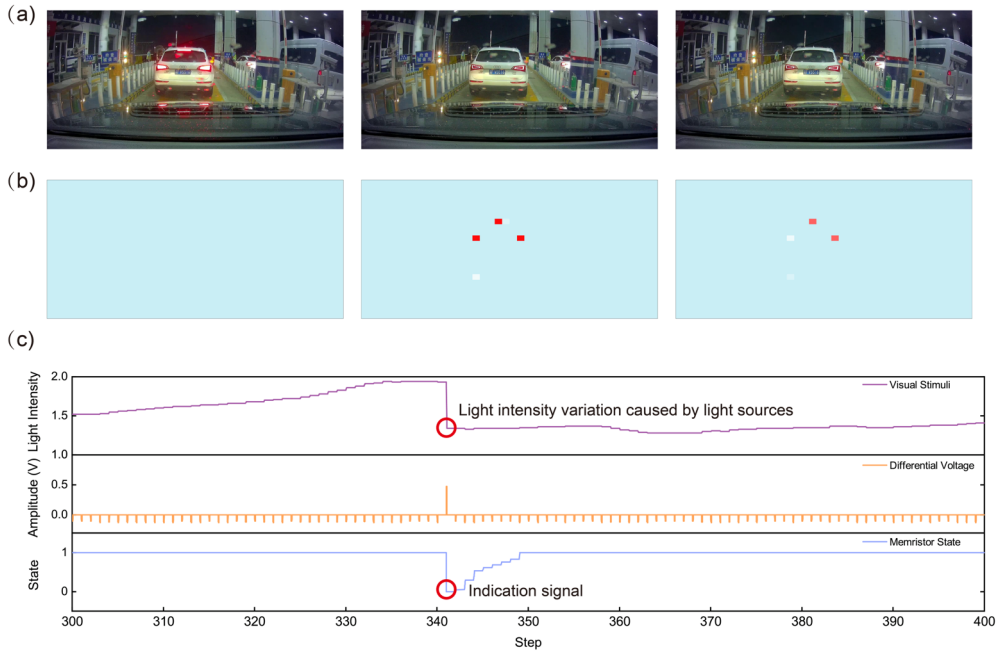

Fig S18. Detection of light sources. (a) Example scenario in the detection of light sources. When the tail lights of a car in the foreground abruptly illuminate or extinguish, a high-frequency change in light intensity ensues. This induces modulation of the memristor into a low-resistance state. (b) The detection results. (c) The light intensity change and its corresponding differential voltage and memristor state.

Fig S19. Analysis of detection performance for moving individuals.

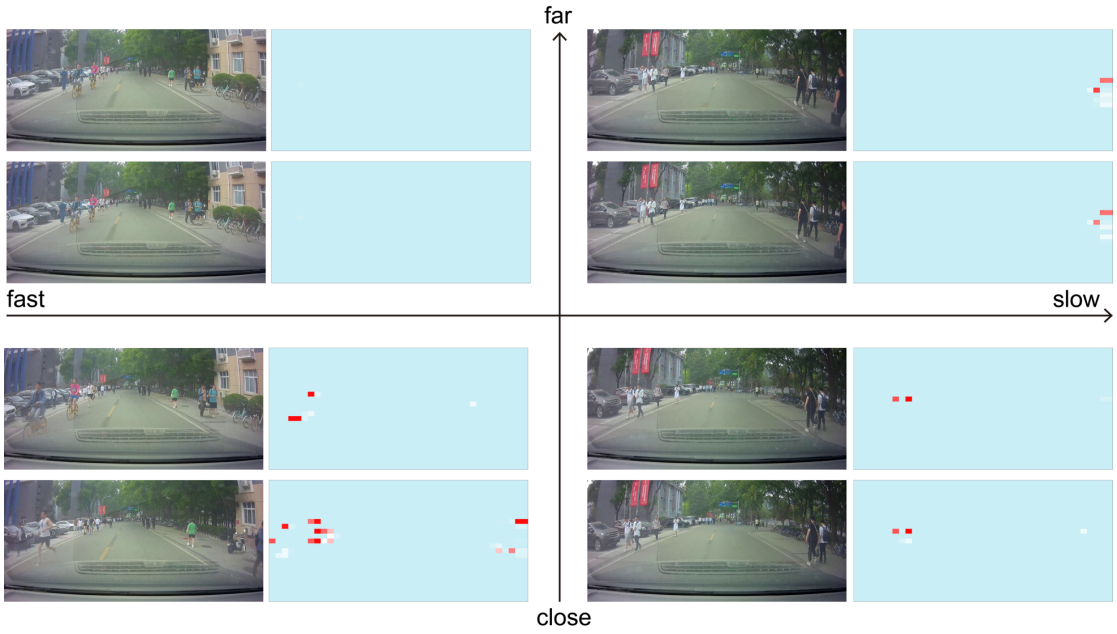

Fig S19. Analysis of detection performance for moving individuals. In the detection of a moving pedestrian, the performance is mainly affected by the position and speed of the pedestrian. Pedestrians are more likely to be detected when they are in close proximity and moving fast.

Fig S20. Detection for extremely hazardous scenarios.

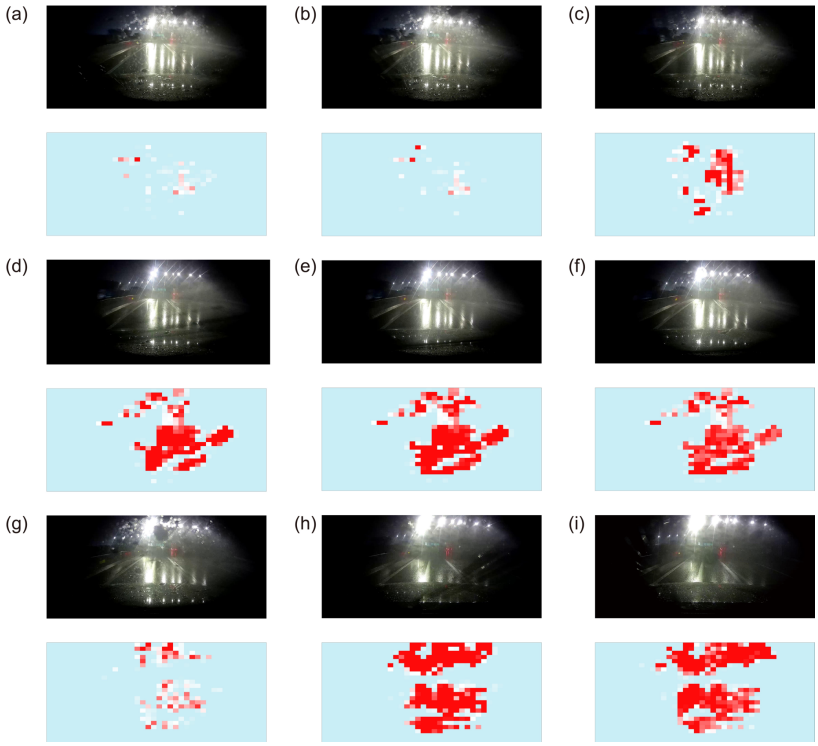

Fig S20. Detection for extremely hazardous scenarios. In certain driving scenarios characterized by abrupt fluctuations in ambient light intensity, depicted in (a) through (i), a significant majority of memristors in the detection results exhibit a low-resistance state. This phenomenon of pervasive low-resistance states can be utilized to characterize challenging driving environments.

Fig S21. The detailed detection results in unstructured environments.

Fig S21. The extended results of Figure 5. In these extended results, more moments are used to reflect the changes in the scene as well as the detection results.

Fig S22. Processing of temperature sensing information.

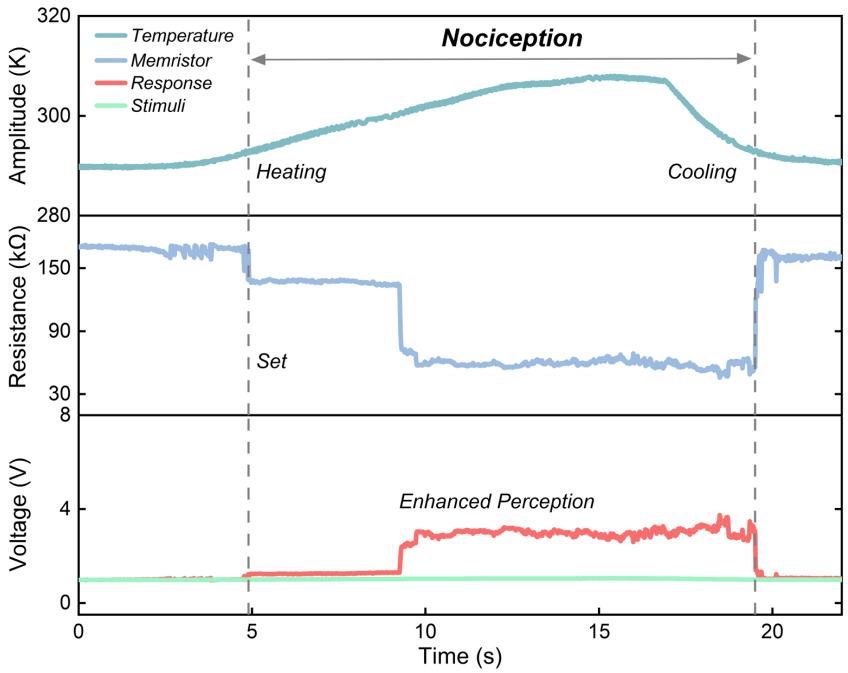

Fig S22. Processing of temperature sensing information. When the environmental temperature increases to exceed the set threshold, the memristor enters the set state with decreasing resistance, producing enhanced perception.

Fig S23. Processing of humidity sensing information.

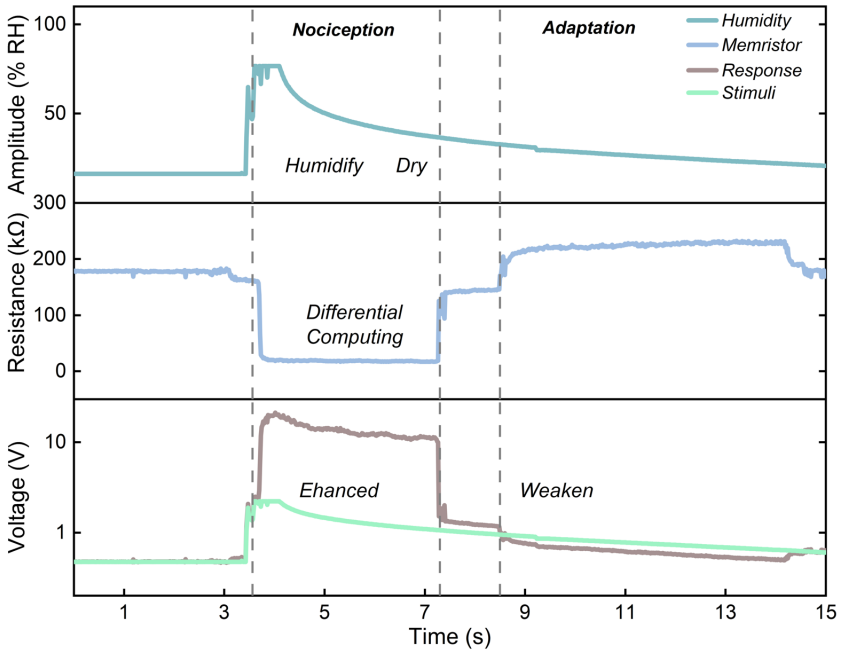

Fig S23. Processing of humidity sensing information. During this experiment, humidity experienced gradual increments and decrements, leading to modulation schemes of nociception, recovery, adaptation, and recovery. Consequently, the memristor states transition sequentially from low-resistance to middle-resistance, then to high-resistance, and back to middle-resistance states. Thus, a single memristor can embody enhanced, adaptation, and normal perception functions through differential computing methods.

Fig S24. The differential processing and learning model.

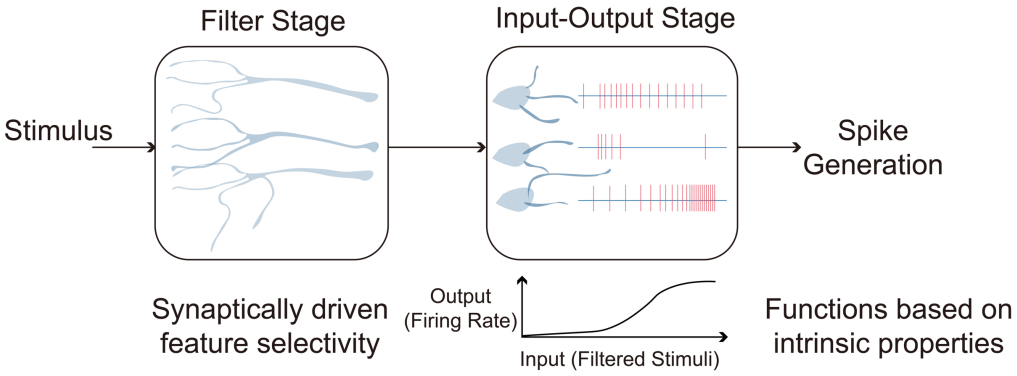

Fig S24. The differential processing and learning model. From perceiving the stimulus to encoding it into neural impulses, the model can be classified into two stages. The first stage can be considered a filter stage where the sensory stimulus is filtered by the feature selectivity of neurons. The second stage can be described as an input-output stage that transforms the filtered stimulus input into a firing rate output. Ultimately, the neural pathways will process these spikes differentially.

Supplementary Tables

Supplementary Table 1 The modulation scheme

Stimulus Strength	Memristor state	Feature pattern	Encoding scheme
$R_p < 60$ kΩ	$R_m > 100$ kΩ	Noxious stimulus	13.3% 0.30 V
$R_p < 60$ kΩ	$R_m < 100$ kΩ	Noxious stimulus	20.0% 0.45 V
60 kΩ < R_p < 100 kΩ	$R_m > 250$ kΩ	Normal stimulus	26.7% 0.35 V
60 kΩ < R_p < 100 kΩ	$R_m < 100$ kΩ	Normal stimulus	20.0% -0.40 V
60 kΩ < R_p < 100 kΩ	180 kΩ < R_m < 250 kΩ	Normal stimulus	6.7% 0.42 V
60 kΩ < R_p < 100 kΩ	100 kΩ < R_m < 160 kΩ	Normal stimulus	6.7% -0.50 V
100 kΩ < R_p < 300 kΩ	$R_m > 100$ kΩ	Mild stimulus	46.7% -0.25 V
100 kΩ < R_p < 300 kΩ	$R_m < 100$ kΩ	Mild stimulus	6.7% -0.50 V
$R_p > 300$ Ko	$R_m > 250$ kΩ	No stimulus	26.7% 0.35 V
$R_p > 300$ kΩ	$R_m < 100$ kΩ	No stimulus	20.0% -0.40 V
$R_p > 300$ kΩ	180 kΩ < R_m < 250 kΩ	No stimulus	6.7% 0.42 V
$R_p > 300$ kΩ	100 kΩ < R_m < 160 kΩ	No stimulus	6.7% -0.50 V

Supplementary Table 2 Comparative Analysis of Visual Information Extraction Algorithm Complexities

Algorithms	Time Complexity	Space Complexity
Gaussian Blur	$O(nmk^2)$	$O(nm)$
Canny Edge Detection	$O(nm)$	$O(nm)$
Histogram Equalization	$O(nmk^2)$	$O(nm)$
SIFT	$O(nm)$	$O(nm)$
SURF	$O(nm)$	$O(nm)$
Our Work	$O(1)$	$O(1)$

Note: m and n are the width and height of the image, respectively, and k is the width of the filter kernel.

Compared to other algorithms, our visual information extraction operates at high speeds in an analog manner and eliminates the need for extra storage space.

List of Supplementary Videos

Supplementary Video SV1 Grasping experiment 1: Sharp object
Supplementary Video SV2 Grasping experiment 2: Slippery object
Supplementary Video SV3 Visual information processing at night
Supplementary Video SV4 Visual information processing in daytime
Supplementary Video SV5 Visual information processing in various driving scenarios
Supplementary Video SV6 Introduction to differential neuromorphic computing

References

1. T. Guan, D. Kothandaraman, R. Chandra, A. J. Sathyamoorthy, K. Weerakoon, D. Manocha, GA-Nav: Efficient terrain segmentation for robot navigation in unstructured outdoor environments. *IEEE Robotics and Automation Letters*. **7**, 8138–8145 (2022).

2. C. Brosque, E. Galbally, O. Khatib, M. Fischer, "Human-robot collaboration in construction: opportunities and challenges" in *2020 International Congress on Human-Computer Interaction, Optimization and Robotic Applications (HORA)* (2020), pp. 1–8.

3. Y. Zhao, Y. Chi, Y. Hong, Y. Li, S. Yang, J. Yin, Twisting for soft intelligent autonomous robot in unstructured environments. *Proceedings of the National Academy of Sciences*. **119**, e2200265119 (2022).

4. M. Beetz, F. Bálint-Benczédi, N. Blodow, D. Nyga, T. Wiedemeyer, Z.-C. Márton, "RoboSherlock: unstructured information processing for robot perception" in *2015 IEEE International Conference on Robotics and Automation (ICRA)* (2015), pp. 1549–1556.

5. T. G. Thuruthel, B. Shih, C. Laschi, M. T. Tolley, Soft robot perception using embedded soft sensors and recurrent neural networks. *Science Robotics*. **4**, eaav1488 (2019).

6. A. Billard, D. Kragic, Trends and challenges in robot manipulation. *Science*. **364**, eaat8414 (2019).

7. R. Deimel, O. Brock, A novel type of compliant and underactuated robotic hand for dexterous grasping. *The International Journal of Robotics Research*. **35**, 161–185 (2016).

8. A. M. Dollar, R. D. Howe, Towards grasping in unstructured environments: grasper compliance and configuration optimization. *Advanced Robotics*. **19**, 523–543 (2005).

9. B. Shih, D. Shah, J. Li, T. G. Thuruthel, Y.-L. Park, F. Iida, Z. Bao, R. Kramer-Bottiglio, M. T. Tolley, Electronic skins and machine learning for intelligent soft robots. *Science Robotics*. **5**, eaaz9239 (2020).

10. F. Liu, S. Deswal, A. Christou, Y. Sandamirskaya, M. Kaboli, R. Dahiya, Neuro-inspired electronic skin for robots. *Science Robotics*. **7**, eabl7344 (2022).

11. F. Liu, S. Deswal, A. Christou, M. Shojaei Baghini, R. Chirila, D. Shakthivel, M. Chakraborty, R. Dahiya, Printed synaptic transistor–based electronic skin for robots to feel and learn. *Science Robotics*. **7**, eabl7286 (2022).

12. V. Ortenzi, M. Controzzi, F. Cini, J. Leitner, M. Bianchi, M. A. Roa, P. Corke, Robotic manipulation and the role of the task in the metric of success. *Nat Mach Intell*. **1**, 340–346 (2019).

13. Z. Li, P. Zhao, C. Jiang, W. Huang, H. Liang, A learning-based model predictive trajectory planning controller for automated driving in unstructured dynamic environments. *IEEE Transactions on Vehicular Technology*. **71**, 5944–5959 (2022).

14. H. Min, X. Xiong, P. Wang, Y. Yu, Autonomous driving path planning algorithm based on improved A* algorithm in unstructured environment. *Proceedings of the Institution of Mechanical Engineers, Part D: Journal of Automobile Engineering*. **235**, 513–526 (2021).

15. Y. Qi, B. He, R. Wang, L. Wang, Y. Xu, Hierarchical motion planning for autonomous vehicles in unstructured dynamic environments. *IEEE Robotics and Automation Letters*. **8**, 496–503 (2023).

16. J.-Q. Yang, R. Wang, Y. Ren, J.-Y. Mao, Z.-P. Wang, Y. Zhou, S.-T. Han, Neuromorphic engineering: from biological to spike-based hardware nervous systems. *Advanced Materials*. **32**, 2003610 (2020).

17. X. Xiao, J. Hu, S. Tang, K. Yan, B. Gao, H. Chen, D. Zou, Recent advances in halide perovskite memristors: materials, structures, mechanisms, and applications. *Advanced Materials Technologies*. **5**, 1900914 (2020).

18. K. Sun, J. Chen, X. Yan, The future of memristors: materials engineering and neural networks. *Advanced Functional Materials*. **31**, 2006773 (2021).

19. Y. G. Song, J. M. Suh, J. Y. Park, J. E. Kim, S. Y. Chun, J. U. Kwon, H. Lee, H. W. Jang, S. Kim, C.-Y. Kang, J. H. Yoon, Artificial adaptive and maladaptive sensory receptors based on a surface-dominated diffusive memristor. *Advanced Science*. **9**, 2103484 (2022).

20. J. Ge, S. Zhang, Z. Liu, Z. Xie, S. Pan, Flexible artificial nociceptor using a biopolymer-based forming-free memristor. *Nanoscale*. **11**, 6591–6601 (2019).

21. C. Zhang, W. B. Ye, K. Zhou, H.-Y. Chen, J.-Q. Yang, G. Ding, X. Chen, Y. Zhou, L. Zhou, F. Li, S.-T. Han, Bioinspired artificial sensory nerve based on nafion memristor. *Advanced Functional Materials*. **29**, 1808783 (2019).

22. J. H. Yoon, Z. Wang, K. M. Kim, H. Wu, V. Ravichandran, Q. Xia, C. S. Hwang, J. J. Yang, An artificial nociceptor based on a diffusive memristor. *Nat Commun*. **9**, 417 (2018).

23. Y. Kim, Y. J. Kwon, D. E. Kwon, K. J. Yoon, J. H. Yoon, S. Yoo, H. J. Kim, T. H. Park, J.-W. Han, K. M. Kim, C. S. Hwang, Nociceptive memristor. *Advanced Materials*. **30**, 1704320 (2018).

24. S. Chen, Z. Lou, D. Chen, G. Shen, An artificial flexible visual memory system based on an UV-motivated memristor. *Advanced Materials*. **30**, 1705400 (2018).

25. C. Jiang, Q. Li, N. Sun, J. Huang, R. Ji, S. Bi, Q. Guo, J. Song, A high-performance bionic pressure memory device based on piezo-OLED and piezo-memristor as luminescence-fish neuromorphic tactile system. *Nano Energy*. **77**, 105120 (2020).

26. Z. Zhang, S. Wang, C. Liu, R. Xie, W. Hu, P. Zhou, All-in-one two-dimensional retinomorphic hardware device for motion detection and recognition. *Nat. Nanotechnol.* **17**, 27–32 (2022).

27. D. Jayachandran, A. Oberoi, A. Sebastian, T. H. Choudhury, B. Shankar, J. M. Redwing, S. Das, A low-power biomimetic collision detector based on an in-memory molybdenum disulfide photodetector. *Nat Electron*. **3**, 646–655 (2020).

28. V. E. Abraira, D. D. Ginty, The sensory neurons of touch. *Neuron*. **79**, 618–639 (2013).

29. A. Lampert, D. L. Bennett, L. A. McDermott, A. Neureiter, E. Eberhardt, B. Winner, M. Zenke, Human sensory neurons derived from pluripotent stem cells for disease modelling and personalized medicine. *Neurobiology of Pain*. **8**, 100055 (2020).

30. E. Kuehn, J. Dinse, E. Jakobsen, X. Long, A. Schäfer, P.-L. Bazin, A. Villringer, M. I. Sereno, D. S. Margulies, Body topography parcellates human sensory and motor cortex. *Cerebral Cortex*. **27**, 3790–3805 (2017).

31. A. Handler, D. D. Ginty, The mechanosensory neurons of touch and their mechanisms of activation. *Nat Rev Neurosci*. **22**, 521–537 (2021).

32. J. del Mármol, M. A. Yedlin, V. Ruta, The structural basis of odorant recognition in insect olfactory receptors. *Nature*. **597**, 126–131 (2021).

33. J. A. Butterwick, J. Del Mármol, K. H. Kim, M. A. Kahlson, J. A. Rogow, T. Walz, V. Ruta, Cryo-EM structure of the insect olfactory receptor Orco. *Nature*. **560**, 447–452 (2018).

34. N. L. Neubarth, A. J. Emanuel, Y. Liu, M. W. Springel, A. Handler, Q. Zhang, B. P. Lehnert, C. Guo, L. L. Orefice, A. Abdelaziz, M. M. DeLisle, M. Iskols, J. Rhyins, S. J. Kim, S. J. Cattel, W. Regehr, C. D. Harvey, J. Drugowitsch, D. D. Ginty, Meissner corpuscles and their spatially intermingled afferents underlie gentle touch perception. *Science*. **368**, eabb2751 (2020).

35. L. L. Tan, R. Kuner, Neocortical circuits in pain and pain relief. *Nat Rev Neurosci*. **22**, 458–471 (2021).

36. K. J. Blake, X. R. Jiang, I. M. Chiu, Neuronal regulation of immunity in the skin and lungs. *Trends in Neurosciences*. **42**, 537–551 (2019).

37. J. Benda, Neural adaptation. *Current Biology*. **31**, R110–R116 (2021).

38. C. R. Donnelly, O. Chen, R.-R. Ji, How do sensory neurons sense danger signals? *Trends in Neurosciences*. **43**, 822–838 (2020).

39. F. Sun, Q. Lu, S. Feng, T. Zhang, Flexible artificial sensory systems based on neuromorphic devices. *ACS Nano*. **15**, 3875–3899 (2021).

40. B. Engelhard, J. Finkelstein, J. Cox, W. Fleming, H. J. Jang, S. Ornelas, S. A. Koay, S. Y. Thiberge, N. D. Daw, D. W. Tank, I. B. Witten, Specialized coding of sensory, motor and cognitive variables in VTA dopamine neurons. *Nature*. **570**, 509–513 (2019).

41. M. M. Iskarous, N. V. Thakor, E-Skins: biomimetic sensing and encoding for upper limb

prostheses. *Proceedings of the IEEE*. **107**, 2052–2064 (2019).

42. B. Wark, B. N. Lundstrom, A. Fairhall, Sensory adaptation. *Current Opinion in Neurobiology*. **17**, 423–429 (2007).

43. F. Liu, S. Deswal, A. Christou, Y. Sandamirskaya, M. Kaboli, R. Dahiya, Neuro-inspired electronic skin for robots. *Sci. Robot.* **7**, eabl7344 (2022).

44. M. Wooten, H.-J. Weng, T. V. Hartke, J. Borzan, A. H. Klein, B. Turnquist, X. Dong, R. A. Meyer, M. Ringkamp, Three functionally distinct classes of C-fibre nociceptors in primates. *Nat Commun*. **5**, 4122 (2014).

45. C.-W. Woo, L. Schmidt, A. Krishnan, M. Jepma, M. Roy, M. A. Lindquist, L. Y. Atlas, T. D. Wager, Quantifying cerebral contributions to pain beyond nociception. *Nat Commun*. **8**, 14211 (2017).

46. A. E. Dubin, A. Patapoutian, Nociceptors: the sensors of the pain pathway. *J Clin Invest*. **120**, 3760–3772 (2010).

47. M. S. Gold, G. F. Gebhart, Nociceptor sensitization in pain pathogenesis. *Nat Med*. **16**, 1248–1257 (2010).

48. A. Handler, D. D. Ginty, The mechanosensory neurons of touch and their mechanisms of activation. *Nat Rev Neurosci*. **22**, 521–537 (2021).

49. A. Zimmerman, L. Bai, D. D. Ginty, The gentle touch receptors of mammalian skin. *Science*. **346**, 950–954 (2014).

50. A. Chortos, J. Liu, Z. Bao, Pursuing prosthetic electronic skin. *Nature Mater*. **15**, 937–950 (2016).

51. L. Spillmann, J. S. Werner, *Visual perception: the neurophysiological foundations* (Elsevier, 2012).

52. C.-H. Sung, J.-Z. Chuang, The cell biology of vision. *Journal of Cell Biology*. **190**, 953–963 (2010).

53. D. Atchison, *Optics of the human eye* (CRC Press, Boca Raton, ed. 2, 2023).